frontiers | Frontiers in Physics

TYPE Original Research
PUBLISHED 11 November 2025
DOI 10.3389/fphy.2025.1713658

OPEN ACCESS

EDITED BY
Fu-Hu Liu,
Shanxi University, China

REVIEWED BY
Muhammad Ajaz,
Abdul Wali Khan University Mardan, Pakistan
Waqas Muhammad,
Hubei University of Automotive Technology, China
Pei-Pin Yang,
Xinzhou Normal University, China

*CORRESPONDENCE
Ying Yuan,
yuany@gxtcmu.edu.cn

RECEIVED 26 September 2025
REVISED 17 October 2025
ACCEPTED 17 October 2025
PUBLISHED 11 November 2025

CITATION
Yuan Y (2025) Kinetic freeze-out properties from transverse momentum spectra of kaon, pion, and (anti-)proton production in U+U collisions at $\sqrt{s_{NN}}$ = 193 GeV.
Front. Phys. 13:1713658.
doi: 10.3389/fphy.2025.1713658

Kinetic freeze-out properties from transverse momentum spectra of kaon, pion, and (anti-)proton production in U+U collisions at $\sqrt{s_{NN}}$ = 193 GeV

Ying Yuan*

Mathematics and Physics Teaching and Research Section, College of Pharmacy, Guangxi University of Chinese Medicine, Nanning, China

In the framework of the multi-source thermal model employing the Tsallis distribution, the transverse momentum distributions of kaon, pion, and (anti-) proton production in U + U collisions at $\sqrt{s_{NN}}$ = 193 GeV with varying centrality are investigated. The transverse momentum spectra are appropriately characterized. The dependencies of parameters (average transverse momenta, effective temperature, and entropy index) on event centrality are determined. It is observed that the q parameters increase as the average number of particles participating in the collisions rises, which implies that the nuclear stopping degree elevates with the increase of collision centrality. The T value remains fundamentally consistent for the same particle under different collision parameters, suggesting that the kinetic freezing temperature of particle ejection in this collision system is independent of the collision parameters. However, the q value exceeded the previously determined research range, which might be related to the deformation of the U-nucleus.

KEYWORDS

transverse momentum distributions, U+U collisions, Tsallis distribution, kinetic freeze-out temperature, $\sqrt{s}$NN= 193 GeV

1 Introduction

Ultra-relativistic heavy-ion collisions (URHICs) provide an unparalleled experimental avenue to explore strongly interacting matter under extreme temperatures and densities–conditions analogous to those prevailing microseconds after the Big Bang [1–7]. A central objective of such studies is to unravel the quantum chromodynamics (QCD) phase structure, particularly the transition from the deconfined quark-gluon plasma (QGP) to the confined hadron gas (HG) [8, 9]. The production mechanisms of hadrons and nuclei in these collisions encode critical signatures of this phase transition, making their investigation pivotal to advancing our understanding of QCD matter. The Relativistic Heavy Ion Collider (RHIC) is uniquely positioned for this research, as it is designed to operate near the critical energy threshold for the hadron-to-QGP phase transition, enabling precise probing of the boundary between these matter states [10].

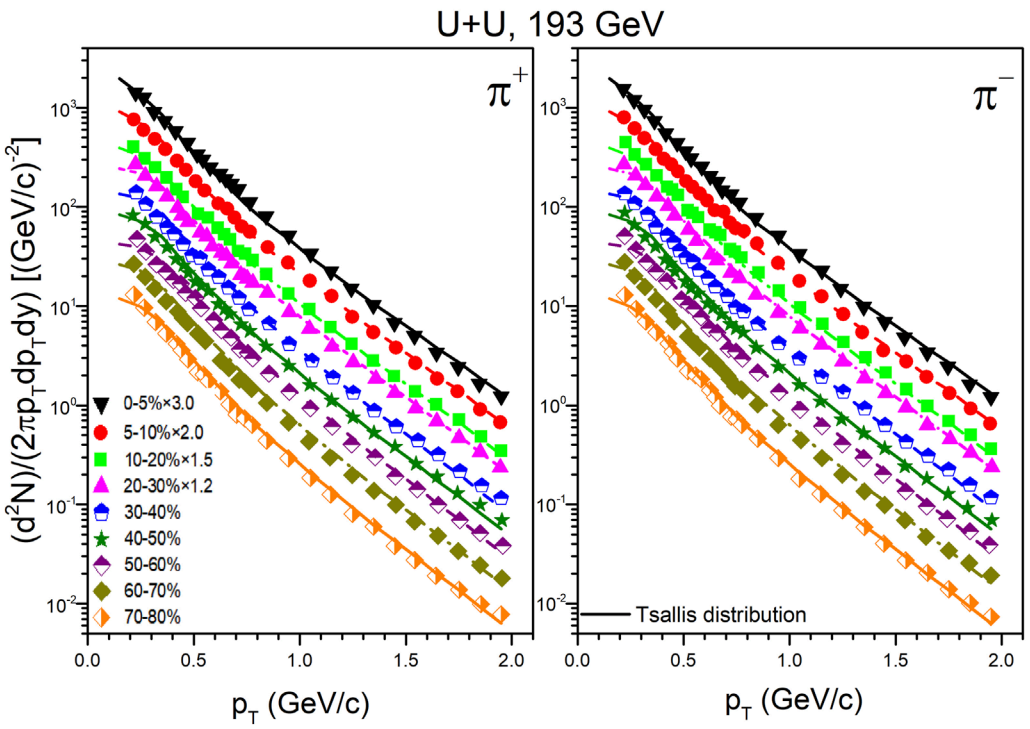

FIGURE 1
Transverse momentum spectra of π^+ and π^- are calculated at mid-rapidity ($|y| < 0.1$) in U + U collisions at $\sqrt{s_{NN}}$ = 193 GeV for 0 – 5%, 5 – 10%, 10 – 20%, 20 – 30%, 30 – 40%, 40 – 50%, 50 – 60%, 60 – 70% and 70 – 80% centrality. The theoretical calculation results based on the Tsallis distribution are represented by lines. Experimental data taken from the STAR Collaboration [21] are represented by the symbols.

Over decades, theoretical frameworks such as the thermal model and coalescence model have been developed to interpret hadron production, offering complementary insights into the evolution of collision systems [11–15]. In particular, the study of transport phenomena is of significant importance for comprehending numerous fundamental properties [16]. Among the most informative observables in URHICs are the transverse momentum spectra of produced particles, which serve as a window into the kinetic freeze-out stage–the point at which hadrons cease strong interactions and their final momenta are fixed [17]. This stage is characterized by key parameters, including the kinetic freeze-out temperature (T_{kin}) and average collective flow velocity, which together reflect the thermal excitation and expansion dynamics of the system [18, 19]. Notably, the "effective temperature" often extracted directly from p_T spectra is not a true thermodynamic temperature but a composite measure encompassing both the system's excitation degree and the contribution of transverse flow [20]. Disentangling these effects to obtain T_{kin}–a fundamental marker of the system's state at freeze-out–remains a core challenge in the field [18].

While extensive studies have probed kinetic freeze-out properties in symmetric, near-spherical heavy-ion systems like Au + Au and Pb + Pb [19], collisions involving highly deformed nuclei such as uranium (U) introduce unique complexities that remain underexplored. The strong deformation of U nuclei modulates the geometric overlap of colliding systems across different centralities,

TABLE 1 Values of T, q, and χ^2/dof corresponding to the curves in U + U collisions for π^+/π^- at $\sqrt{s_{NN}}$ = 193 GeV for 0 – 5%, 5 – 10%, 10 – 20%, 20 – 30%, 30 – 40%, 40 – 50%, 50 – 60%, 60 – 70% and 70 – 80% centrality.

Figure	Type 1	Type 2	T (GeV)	q	χ^2/dof
Figure 1	π^+/π^-	0%–5%	0.075 ± 0.042	1.288 ± 0.100	0.010
		5%–10%	0.077 ± 0.018	1.280 ± 0.068	0.004
		10%–20%	0.079 ± 0.005	1.272 ± 0.014	0.006
		20%–30%	0.081 ± 0.035	1.268 ± 0.160	0.010
		30%–40%	0.080 ± 0.008	1.258 ± 0.357	0.006
		40%–50%	0.079 ± 0.008	1.263 ± 0.356	0.008
		50%–60%	0.081 ± 0.008	1.258 ± 0.339	0.013
		60%–70%	0.079 ± 0.037	1.258 ± 0.137	0.032
		70%–80%	0.078 ± 0.032	1.258 ± 0.086	0.007

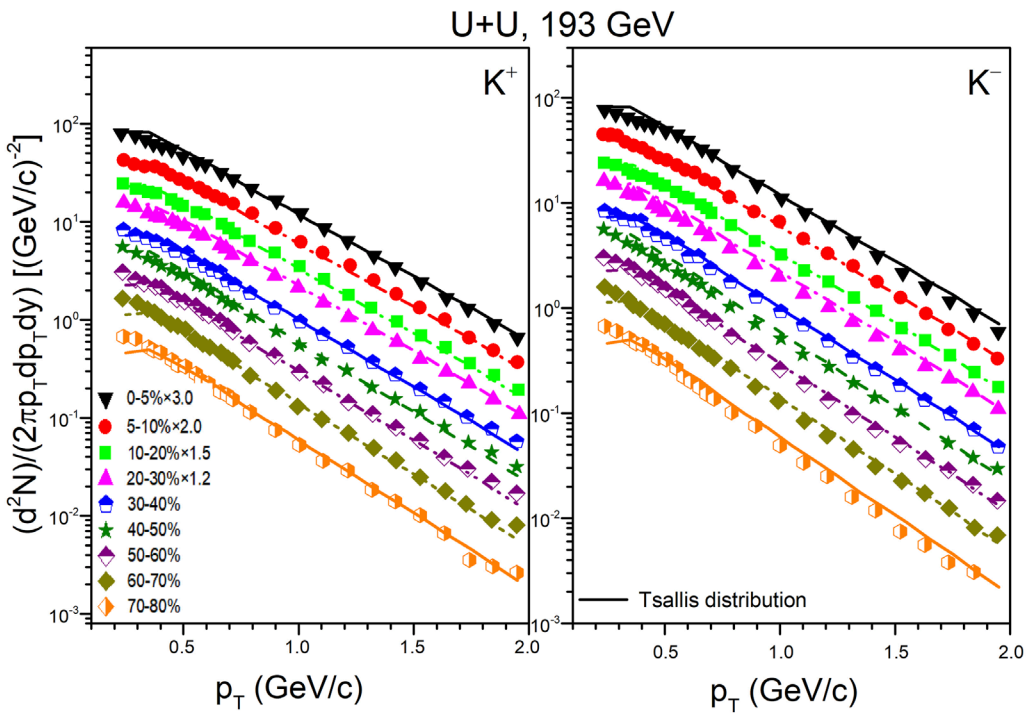

FIGURE 2
Transverse momentum spectra of k^+ and k^- are calculated at mid-rapidity ($|y| < 0.1$) in U + U collisions at $\sqrt{s_{NN}}$ = 193 GeV for 0 – 5%, 5 – 10%, 10 – 20%, 20 – 30%, 30 – 40%, 40 – 50%, 50 – 60%, 60 – 70% and 70 – 80% centrality. The theoretical calculation results based on the Tsallis distribution are represented by lines. Experimental data taken from the STAR Collaboration [21] are represented by the symbols.

TABLE 2 Values of T, q, and χ^2/dof corresponding to the curves in U + U collisions for k^+/k^- at $\sqrt{s_{NN}}$ = 193 GeV for 0 – 5%, 5 – 10%, 10 – 20%, 20 – 30%, 30 – 40%, 40 – 50%, 50 – 60%, 60 – 70% and 70 – 80% centrality.

Figure	Type 1	Type 2	T (GeV)	q	χ^2/dof
Figure 2	k^+/k^-	0%–5%	0.098 ± 0.030	1.308 ± 0.269	0.016
		5%–10%	0.100 ± 0.015	1.300 ± 0.068	0.005
		10%–20%	0.100 ± 0.048	1.292 ± 0.102	0.006
		20%–30%	0.102 ± 0.009	1.288 ± 0.356	0.021
		30%–40%	0.100 ± 0.015	1.284 ± 0.068	0.006
		40%–50%	0.098 ± 0.012	1.278 ± 0.060	0.026
		50%–60%	0.100 ± 0.013	1.278 ± 0.056	0.021
		60%–70%	0.100 ± 0.018	1.270 ± 0.004	0.038
		70%–80%	0.102 ± 0.013	1.260 ± 0.076	0.023

potentially altering nuclear stopping, collective flow, and ultimately freeze-out dynamics [21].

This study is motivated by the need to leverage this new experimental data to extract reliable kinetic freeze-out temperatures for U + U collisions. We employ the Tsallis distribution–renowned for its ability to capture non-equilibrium features of high-energy collision systems [22–24] –within the multi-source thermal model, a framework well-suited to describing the multi-component emission of hadrons. By simulating the p_T distributions of kaons, pions, and (anti-)protons and comparing our results with STAR's experimental data [21], we aim to quantify T_{kin} and its dependence on collision centrality. Beyond extracting this key parameter, our work seeks to lay the groundwork for comparing freeze-out properties between deformed U + U and spherical Au + Au systems, offering insights into how nuclear deformation influences the late-stage evolution of QCD matter.

2 The model and methods

The model employed in the current study is the multi-source thermal model [25–27]. In this model, numerous emission sources are formed during high - energy nucleus - nucleus collisions. Various distributions can be utilized to characterize the emission sources and particle spectra, including the Tsallis distribution, the standard (Boltzmann, Fermi - Dirac, and Bose - Einstein) distributions, the Tsallis + standard distributions [28–33], the Erlang distribution [25],

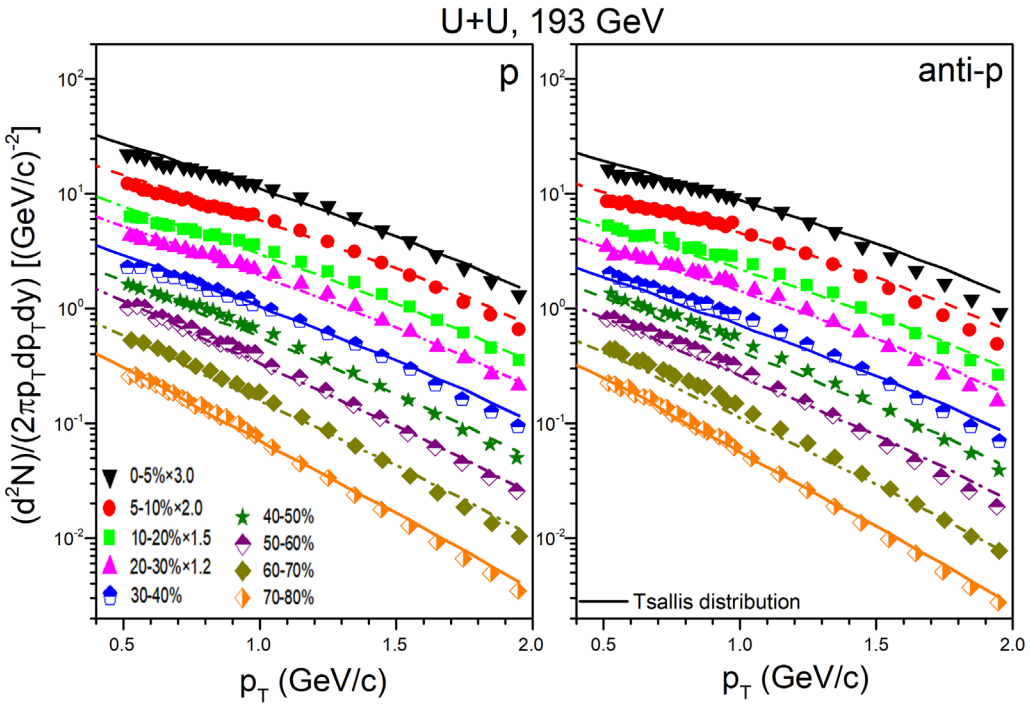

FIGURE 3
The transverse momentum spectra of p and $\bar{p}$ are computed at mid-rapidity ($|y| < 0.1$) in $U+U$ collisions at $\sqrt{s_{NN}}$ = 193 GeV for centrality intervals of 0 – 5%, 5 – 10%, 10 – 20%, 20 – 30%, 30 – 40%, 40 – 50%, 50 – 60%, 60 – 70% and 70 – 80%. The theoretical calculation results based on the Tsallis distribution are represented by lines. The experimental data sourced from the STAR Collaboration [21] are denoted by the symbols.

etc.,.The Tsallis distribution can be depicted by two or three standard distributions.

The experimental data of the transverse momentum spectrum of the particles are fitted using the Tsallis distribution, which can account for the temperature fluctuation in several sources to yield an average value. The Tsallis distribution exhibits multiple functional forms [22–24, 28–35], among which the normalized standard momentum distribution relying on the Boltzmann distribution can be expressed as

$$f(p) = \frac{1}{N}\frac{dN}{dp} = Cp^2\left\{\left[1 \pm \frac{q-1}{T}\left(\sqrt{p^2+m_0^2}-\mu\right)\right]^{\pm\frac{1}{q-1}}\right\}^{-1}. \quad (1)$$

Here, N represents the particle number, C is the normalization constant, m_0 is the rest mass of the studied particle, T is the temperature that averagely describes several sources (local equilibrium states), q is the entropy index which describes the degree of non-equilibrium among different states, μ is the chemical potential related to $\sqrt{s_{NN}}$ [36].

In the rest frame of a considered source, a simplified form of the joint probability is selected: density function of transverse momentum (p_T) and rapidity (y) [10],

$$f(p_T,y) \propto \frac{d^2N}{dydp_T} = \frac{gV}{(2\pi)^2}p_T\sqrt{p_T^2+m_0^2}\cosh y \times \left[1 \pm \frac{q-1}{T}\left(\sqrt{p_T^2+m_0^2}\cosh y - \mu\right)\right]^{\pm\frac{q}{q-1}}. \quad (2)$$

Here, g is the degeneracy factor, V is the volume of emission sources. In the RHIC energy region, μ is very small, the ± in the formula takes the plus sign. The values of T, q and V are obtained from reproducing the particle spectra, where T and q are independently fitted for the studied particle, and V is related to other parameters.

The Monte Carlo distribution generating method is adopted to obtain p_T. Let r_1 denote the random numbers uniformly distributed in [0,1]. A series of values of p_T can be acquired through:

$$\int_0^{p_T} f_{p_T}(p_T)\,dp_T < r_1 < \int_0^{p_T+dp_T} f_{p_T}(p_T)\,dp_T. \quad (3)$$

Here, f_{p_T} is the transverse momentum probability density function, which is an alternative representation of the Tsallis distribution as follows:

$$f_{p_T}(p_T) = \frac{1}{N}\frac{dN}{dp_T} = \int_{y_{min}}^{y_{max}} f(p_T,y)\,dy. \quad (4)$$

where y_{max} and y_{min} are the maximum and minimum rapidity, respectively.

Under the assumption of isotropic emission in the source rest frame, the Monte Carlo method is used to obtain the polar angle:

$$\theta = 2\arcsin\sqrt{r_2}. \quad (5)$$

Thus, a series of values of momentum and energy can be obtained based on the momentum $p = \frac{p_T}{\sin\theta}$ and the energy $E = \sqrt{p^2+m_0^2}$. Therefore, the corresponding values of rapidity can be derived according to the definition of rapidity.

TABLE 3 Values of T, q, and χ^2/dof corresponding to the curves in U + U collisions for p and $\bar{p}$ at $\sqrt{s_{NN}}$ = 193 GeV for 0 – 5%, 5 – 10%, 10 – 20%, 20–30%, 30 – 40%, 40 – 50%, 50 – 60%, 60 – 70% and 70 – 80% centrality.

Figure	Type 1	Type 2	T (GeV)	q	χ^2/dof
Figure 3	p	0%–5%	0.102 ± 0.014	1.418 ± 0.485	0.011
		5%–10%	0.102 ± 0.023	1.414 ± 0.072	0.007
		10%–20%	0.100 ± 0.042	1.409 ± 0.132	0.021
		20%–30%	0.102 ± 0.021	1.394 ± 0.111	0.022
		30%–40%	0.102 ± 0.010	1.384 ± 0.081	0.010
		40%–50%	0.100 ± 0.016	1.370 ± 0.055	0.009
		50%–60%	0.100 ± 0.003	1.345 ± 0.037	0.004
		60%–70%	0.100 ± 0.020	1.335 ± 0.064	0.008
		70%–80%	0.100 ± 0.018	1.305 ± 0.081	0.006
Figure 3	$\bar{p}$	0%–5%	0.103 ± 0.022	1.442 ± 0.081	0.042
		5%–10%	0.103 ± 0.012	1.435 ± 0.140	0.022
		10%–20%	0.103 ± 0.025	1.425 ± 0.165	0.015
		20%–30%	0.103 ± 0.020	1.415 ± 0.149	0.015
		30%–40%	0.102 ± 0.005	1.400 ± 0.076	0.021
		40%–50%	0.102 ± 0.013	1.375 ± 0.088	0.021
		50%–60%	0.102 ± 0.007	1.355 ± 0.031	0.019
		60%–70%	0.102 ± 0.008	1.325 ± 0.282	0.025
		70%–80%	0.102 ± 0.002	1.295 ± 0.079	0.027

3 Results and discussion

3 1 Transverse momentum spectra

Figure 1 depicts the transverse momentum spectra within nine centrality classes in U + U collisions at $\sqrt{s_{NN}}$ = 193 GeV at mid-rapidity ($|y| < 0.1$) for π^+ and π^-. There exist nine centrality classes, representing ranges of 0 – 5%, 5 – 10%, 10 – 20%, 20 – 30%, 30 – 40%, 40 – 50%, 50 – 60%, 60 – 70% and 70 – 80% respectively. The symbols denote the experimental data from the STAR Collaboration [21]. The lines represent our calculated results fitted by utilizing the Tsallis distribution based on Equation 2 in the mid-rapidity region. The values of the relevant parameters T and q are presented in Table 1, along with χ^2/dof (where χ^2 is the chi-square value and dof is the number of degrees of freedom). It is observed that the calculations from the Tsallis distribution are in good agreement with the experimental data.

Figure 2 illustrates the transverse momentum spectra across nine centrality classes in U + U collisions at $\sqrt{s_{NN}}$ = 193 GeV at mid-rapidity ($|y| < 0.1$) for k^+ and k^-. The lines are the results computed from the Tsallis distribution. The symbols represent the experimental data of the STAR Collaboration [21]. The values of the relevant parameters T and q are given in Table 2, along with χ^2/dof. It is found that the calculations of the Tsallis distribution are in good accordance with the experimental data.

Figure 3 presents the transverse momentum spectra for nine centrality classes in U + U collisions at $\sqrt{s_{NN}}$ = 193 GeV, measured at mid-rapidity ($|y| < 0.1$) for protons (p) and antiprotons ($\bar{p}$). The lines are the results obtained from the Tsallis distribution. The symbols represent the experimental data of the STAR Collaboration [21]. The values of the related parameters T and q are provided in Table 3, along with χ^2/dof. It is noted that the calculations of the Tsallis distribution are in good conformity with the experimental data.

Under normal conditions, the q value value lies between 1.0 and 1.2; however, the q values in the above tables exceed this range [37]. Given that the U nucleus is the most deformed nucleus, the correction for nuclear deformation is not considered in the current Tsallis distribution, thus resulting in a relatively large q value. The T value remains essentially consistent under different collision centrality, which is attributable to the fact that the orientation of the U nucleus is isotropic in the calculation.

3.2 Average transverse momenta distributions

Figure 4 shows the variation of $\langle p_T \rangle$ with $\langle N_{part} \rangle$ at mid-rapidity ($|y| < 0.1$) for π^+, k^+ and p particles in U + U collisions at $\sqrt{s_{NN}}$ = 193 GeV. The red solid circles represent the experimental data

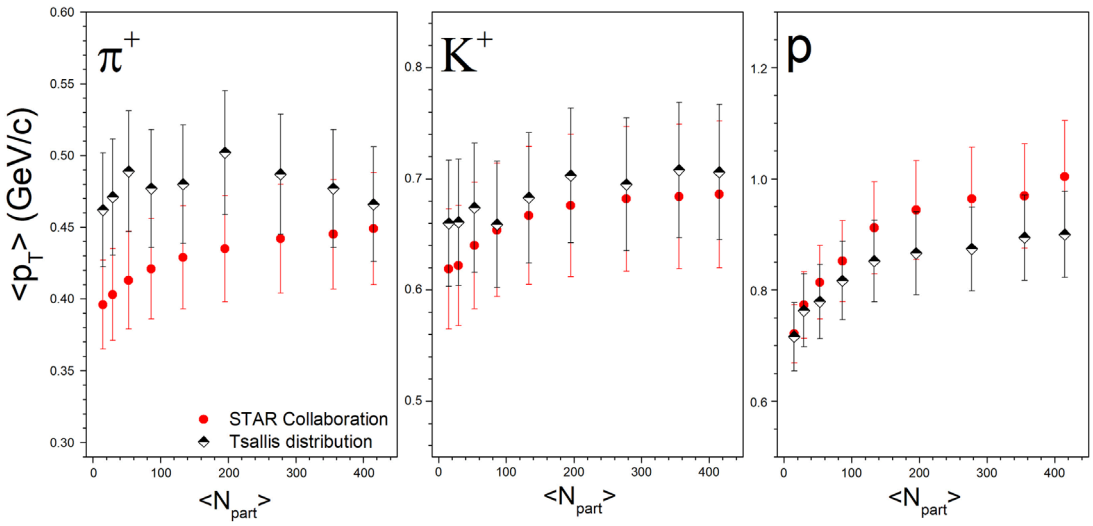

FIGURE 4
The $\langle p_T \rangle$ as a function of $\langle N_{part} \rangle$ at mid-rapidity ($|y| < 0.1$) of π^+, k^+ and p for $U+U$ collisions at $\sqrt{s_{NN}}$ = 193 GeV. The red solid circles represent data collected by the STAR Collaboration [21]. The black diamonds represent the calculations based on the Tsallis distribution.

TABLE 4 Values of $\langle p_T \rangle$ in GeV/c within mid-rapidity ($|y| < 0.1$) of π^+, π^-, k^+, k^-, p and $\bar{p}$ for U + U collisions at $\sqrt{s_{NN}}$ = 193 GeV using the Tsallis distribution.

Centrality	π^+	π^-	k^+	k^-	p	$\bar{p}$
0%–5%	0.466 ± 0.040	0.466 ± 0.040	0.706 ± 0.061	0.706 ± 0.061	0.900 ± 0.077	0.938 ± 0.081
5%–10%	0.477 ± 0.041	0.477 ± 0.041	0.708 ± 0.061	0.708 ± 0.061	0.894 ± 0.077	0.929 ± 0.080
10%–20%	0.487 ± 0.042	0.487 ± 0.042	0.695 ± 0.060	0.695 ± 0.060	0.874 ± 0.075	0.916 ± 0.079
20%–30%	0.502 ± 0.043	0.502 ± 0.043	0.703 ± 0.060	0.703 ± 0.060	0.866 ± 0.074	0.902 ± 0.078
30%–40%	0.480 ± 0.041	0.480 ± 0.041	0.683 ± 0.059	0.683 ± 0.059	0.852 ± 0.073	0.875 ± 0.075
40%–50%	0.477 ± 0.041	0.477 ± 0.041	0.659 ± 0.057	0.659 ± 0.057	0.817 ± 0.070	0.838 ± 0.072
50%–60%	0.489 ± 0.042	0.489 ± 0.042	0.674 ± 0.058	0.674 ± 0.058	0.779 ± 0.067	0.808 ± 0.069
60%–70%	0.471 ± 0.041	0.471 ± 0.041	0.661 ± 0.057	0.661 ± 0.057	0.763 ± 0.066	0.762 ± 0.066
70%–80%	0.462 ± 0.040	0.462 ± 0.040	0.660 ± 0.057	0.660 ± 0.057	0.716 ± 0.062	0.714 ± 0.061

from the STAR Collaboration [21], and the black diamonds are the calculations from the Tsallis distribution. The calculations can be derived by

$$\langle p_T \rangle = \frac{\sum p_{T1} \alpha}{\sum \alpha}. \quad (6)$$

Here, p_{T1} is the value of transverse momentum corresponding to the experimental data, and α is the value of $\frac{d^2N}{N_{event} 2\pi p_T dp_T dy}$ that corresponds to the p_{T1}. It is found that the experimental results can be described within the margin of error. The values of $\langle p_T \rangle$ increase gradually with the increase of number of participating nucleons, and they are listed in Table 4. In other words, the greater the intensity of the collision, the higher the transverse momentum of the emitted particles.

3.3.Dependence of parameters on number of participating nucleons

Figures 5, 6 illustrate the variation trends of parameters (T and q) with the average number of participants for $\pi(\pi^+/\pi^-)$, $k(k^+/k^-)$, p and $\bar{p}$ generated in $U+U$ collisions at $\sqrt{s_{NN}}$ = 193 GeV in the mid-rapidity region ($|y| < 0.1$). The symbols denote the parameter values extracted from Figures 1–3 and listed in Tables 1–3.

From Figures 5, 6, it can be observed that the T value remains relatively stable for the same particle, whereas the q value increases as the collision centrality rises. In high-energy experiments, the tip-to-tip collisions and body-to-body collisions of the U nucleus exhibit distinctly different characteristics. However, a slight mass hierarchy phenomenon was also observed: protons (and anti-protons) exhibited the highest T value, followed by k mesons, with π

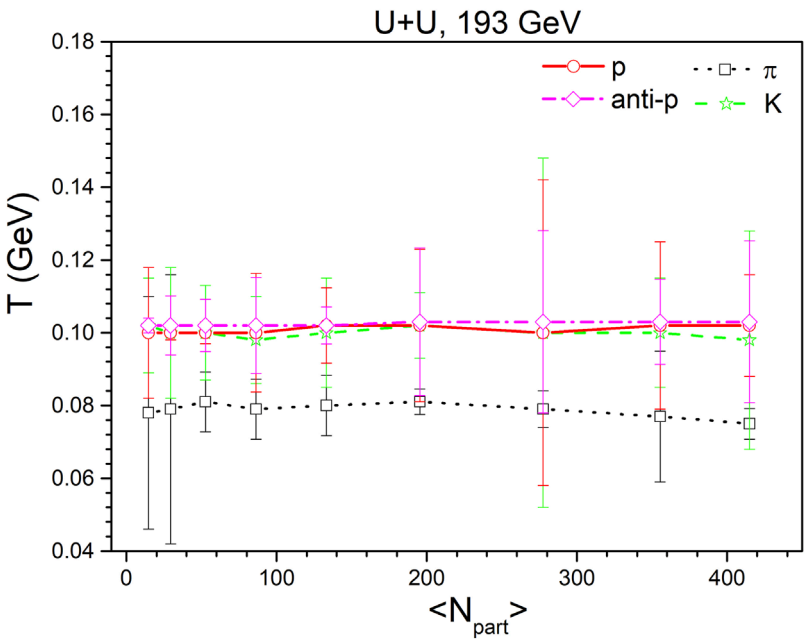

FIGURE 5
Dependence of T on the average number of participants for π^+/π^-, k^+/k^-, p and $\bar{p}$ in events with different centrality intervals. The symbols represent the parameter values listed in Tables 1–3.

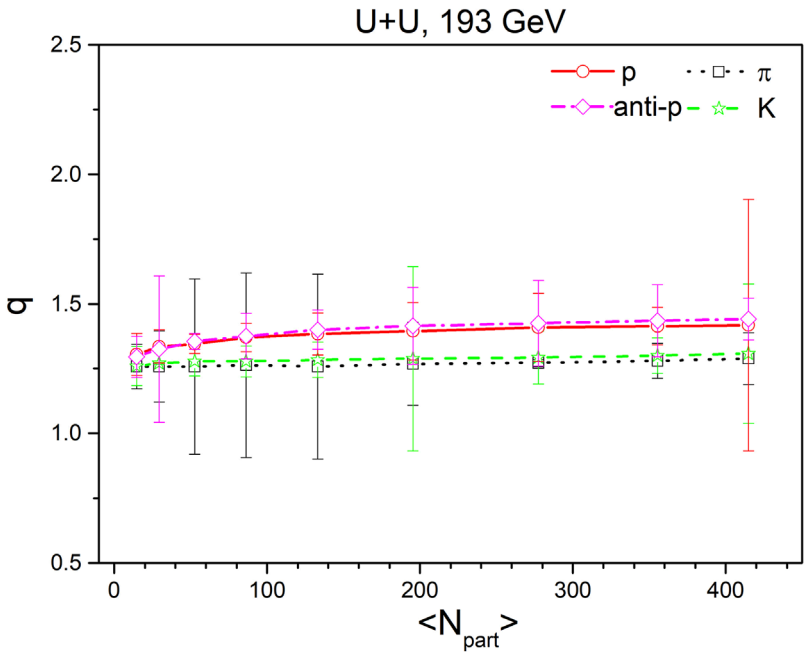

FIGURE 6
Dependence of q on the average number of participants for π^+/π^-, k^+/k^-, p and $\bar{p}$ in events with different centrality intervals. The symbols represent the parameter values listed in Tables 1–3.

mesons displaying the lowest. The q value also shows a dependence on the mass of the particle. This trend can be attributed to the fact that heavier particles, such as protons, more efficiently acquire kinetic energy from the system's collective expansion, leading to a harder transverse momentum spectrum and consequently a higher fitted effective temperature T. The closer to the center of the collision, the higher the temperature generated by the fireball, the greater the energy density, and the more significant the non-equilibrium characteristics of the system are usually, thus having a higher entropy value.

4. Summary and outlook

In conclusion, within the centrality classes of 0 – 5%, 5 – 10%, 10 – 20%, 20 – 30%, 30 – 40%, 40 – 50%, 50 – 60%, 60 – 70%, and 70 – 80% in $U + U$ collisions at $\sqrt{s_{NN}}$ = 193 GeV,the transverse momentum spectra of $\pi^{\pm}$, $k^{\pm}$, and $p(\bar{p})$ in mid-rapidity region ($|y| < 0.1$) were measured. Additionally, other observable extracted from the transverse momentum spectra, such as the average transverse momentum ($\langle p_T \rangle$), and the relationships regarding effective temperature and entropy are presented as functions of collision centrality. The experimental results from the STAR Collaboration [21] were analyzed using the Tsallis distribution. It was found that the theoretical calculation results can effectively describe the experimental data, and the function of $\langle p_T \rangle$ depends on centrality. The T value remains basically consistent for the same particle under different collision parameters. The q value increases as the collision parameters decrease, yet it exceeds the previously determined research scope. Subsequently, in-depth research will examine Tsallis distribution corrections in deformed nuclei. Further studies on the kinetic freeze-out temperature and collision time evolution are still needed.

Data availability statement

The original contributions presented in the study are included in the article/supplementary material, further inquiries can be directed to the corresponding author.

Author contributions

YY: Writing – review and editing, Writing – original draft.

Funding

The author(s) declare that financial support was received for the research and/or publication of this article. This work was supported by the Fund for Less Developed Regions of the National Natural Science Foundation of China under Grant No.12365017, the Natural Science Foundation of Guangxi Zhuangzu Autonomous Region of China under Grant No. 2021GXNSFAA196052, the Introduction of Doctoral Starting Funds of Scientific Research of Guangxi University of Chinese Medicine under Grant No.2018BS024.

Conflict of interest

The author declares that the research was conducted in the absence of any commercial or financial relationships that could be construed as a potential conflict of interest.

Generative AI statement

The author(s) declare that no Generative AI was used in the creation of this manuscript.

Any alternative text (alt text) provided alongside figures in this article has been generated by Frontiers with the support of artificial intelligence and reasonable efforts have been made to ensure accuracy, including review by the authors wherever possible. If you identify any issues, please contact us.

Publisher's note

References

1. Alt T, Anticic B, Baatar D, Barna J, Betev L. Energy dependence of Λ and Ξ production in central pb+Pb collisions at 20A, 30A, 40A, 80A,and 158A GeV measured at the CERN super proton synchrotron. *Phys Rev C* (2008) 78(3):034918. doi:10.1103/PhysRevC.78.034918

2. Sun JX, Liu FH, Wang EQ. Pseudorapidity distributions of charged particles and contributions of leading nucleons in Cu-Cu collisions at high energies. *Chin Phys Lett* (2010) 27(3):032503. doi:10.1088/0256-307x/27/3/032503

3. Wang EQ, Liu FH, Rahim MA, Fakhraddin S, Sun JX. Singly and doubly charged projectile fragments in nucleus-emulsion collisions at dubna energy in the framework of the multi-source model. *Chin Phys Lett* (2011) 28(8):082501. doi:10.1088/0256-307x/28/8/082501

4. Li BC, Huang M. Strongly coupled matter near phase transition. *J Phys G-Nuclear Part Phys* (2009) 36(6):064062. doi:10.1088/0954-3899/36/6/064062

5. Li LL, Liu FH. Kinetic freeze-out properties from transverse momentum spectra of pions in high energy proton-proton collisions. *Physics* (2020) 2020(2):277–308. doi:10.3390/physics2020015

6. Alrebdi HI, Ajaz M, Badshah M, Waqas M, Alsaif NAM, Ahmad MA, et al. Thermal freeze-out and collective signatures in collisions with a non-extensive statistical study on energy and pseudorapidity systematics. *Scientific Rep* (2025) 15:27194. doi:10.1038/s41598-025-08380-w

7. Abdulameer NJ. Identified charged-hadron production in p+Al, ^3He + *Au*, and cu+Au collisions at GeV and in U+U collisions at GeV. *Phys Rev C* (2024) 109:054910. doi:10.1103/PhysRevC.109.054910

8. Arsenescu R, Baglin C, Beck HP, Borer K, Bussière A, Elsener K, et al. An investigation of the antinuclei and nuclei production mechanism in Pb + Pb collisions at 158 A GeV. *New J Phys* (2003) 5:150. doi:10.1088/1367-2630/5/1/150

9. Li QF, Wang YJ, Wang XB, Shen CW. Helium-3 production from pb+Pb collisions at SPS energies with the UrQMD model and the traditional coalescence afterburner. *Sci China: Phys Mech Astron* (2016) 59(3):632002. doi:10.1007/s11433-015-5775-3

10. Lao HL, Wei HR, Liu FH, Lacey RA. An evidence of mass-dependent differential kinetic freeze-out scenario observed in Pb-Pb collisions at 2.76 TeV. *The Eur Phys J A* (2016) 52:203. doi:10.1140/epja/i2016-16203-2

11. Mrowczynski S, Slon P. Hadron-deuteron correlations and production of light nuclei in relativistic heavy-ion collisions. *Acta Physica Pol B* (2020) 51(8):1739–55. doi:10.5506/aphyspolb.51.1739

12. Mrowczynski S. Production of light nuclei in the thermal and coalescence models. *Acta Physica Pol B* (2017) 48(4):707–16. doi:10.5506/aphyspolb.48.707

13. Mrowczynski S, Mrówczyński S. He *versus* li and production of light nuclei in relativistic heavy-ion collisions. *Mod Phys Lett A* (2018) 33(25):1850142. doi:10.1142/s0217732318501420

14. Liu P, Chen JH, Ma YG, Zhang S. Production of light nuclei and hypernuclei at high intensity accelerator facility energy region. *Nucl Sci Tech* (2017) 28(4):55. doi:10.1007/s41365-017-0207-x

15. Liu FX, Chen G, Zhe ZL, Zhou DM, Xie YL. Light (anti)nuclei production in cu+Cu collisions at 200 GeV. *The Eur Phys J A* (2019) 55:160. doi:10.1140/epja/i2019-12851-x

16. Li BC, Fu YY, Wang LL, Liu FH. Dependence of elliptic flows on transverse momentum and number of participants in au+Au collisions at = 200 GeV. *J Phys G-Nuclear Part Phys* (2013) 40(2):025104. doi:10.1088/0954-3899/40/2/025104

17. Chen YH, Liu FH, Sarkisyan-Grinbaum EK. Event patterns from negative Pion spectra in proton-proton and nucleus-nucleus collisions at SPS. *Chin Phys C* (2018) 42(10):104102. doi:10.1088/1674-1137/42/10/104102

18. Waqas M, Peng G-X, Ajaz M, Haj Ismail A, Wazir Z, Li L-L. Extraction of different temperatures and kinetic freeze-out volume in high energy collisions. *J Phys G: Nucl Part Phys* (2022) 49:095102. doi:10.1088/1361-6471/ac6a00

19. Kumar L. Systematics of kinetic freeze-out properties in high EnergyCollisions from STAR. *Nucl Phys A* (2014) 931:1114–9. doi:10.1016/j.nuclphysa.2014.08.085

20. Waqas M, Liu FH, Li LL, Mas Alfanda H. Effective (kinetic freeze-out) temperature, transverse flow velocity, and kinetic freeze-out volume in high energy collisions. *Nucl Sci Tech* (2020) 31:109. doi:10.1007/s41365-020-00821-7

21. Abdallah MS. Pion, kaon, and (anti) proton production in U+U collisions at =193 GeV measured with the STAR detector. *Phys Rev C* (2023) 107:024901. doi:10.1103/PhysRevC.107.024901

22. Tsallis C. Possible generalization of boltzmann-gibbs statistics. *J Stat Phys* (1988) 52(1-2):479–87. doi:10.1007/bf01016429

23. Biró TS, Purcsel G, Ürmössy K. Non-extensive approach to quark matter. *The Eur Phys J A* (2009) 40(3):325. doi:10.1140/epja/i2009-10806-6

24. Cleymans J, Worku D. Relativistic thermodynamics: transverse momentum distributions in high-energy physics. *The Eur Phys J A* (2012) 48(11):160. doi:10.1140/epja/i2012-12160-0

25. Liu FH, Gao YQ, Wei HR. On descriptions of particle transverse momentum spectra in high energy collisions. *Adv High Energy Phys* (2014):293873. doi:10.1155/2014/293873

26. Liu FH, Gao YQ, Tian T, Li BC. Unified description of transverse momentum spectrums contributed by soft and hard processes in high-energy nuclear collisions. *Eur Phys J A* (2014) 50(6):94. doi:10.1140/epja/i2014-14094-9

27. Liu FH, Li JS. Isotopic production cross section of fragments in ^{56}Fe+p and $^{136}Xe(^{124}Xe)$+Pb reactions over an energy range from 300 A to 1500 A MeV. *Phys Rev C* (2008) 78(4):044602. doi:10.1103/physrevc.78.044602

28. Zhang PC, Yang PP, Duan TT, Zhu HL, Liu FH, Olimov KK. Comparing effective temperatures in standard and Tsallis distributions from transverse momentum spectra in small collision systems. *Indian J Phys* (2025). doi:10.1007/s12648-025-03742-6

29. Duan TT, Yang PP, Zhang PC, Lao HL, Liu FH, Olimov KK. Comparing effective temperatures in standard, tsallis, and q-dual statistics from transverse momentum spectra of identified light charged hadrons produced in gold–gold collisions at RHIC energies. *Eur Phys J Plus* (2024) 139:1069. doi:10.1140/epjp/s13360-024-05853-1

30. Bhattacharyya T, Rybczyński M, Wilk G, Włodarczyk Z. A harmonic oscillator in nonadditive statistics and a novel transverse momentum spectrum in high-energy collisions. *Phys Lett B* (2025) 867:139588. doi:10.1016/j.physletb.2025.139588

31. Waqas M, Khan HA, Bietenholz W, Ajaz M, Slimane JB, Alrebdi HI, et al. Thermodynamic analysis of transverse momentum spectra in Pb–Pb collisions at 2.76 TeV: centrality dependence of temperature, freezeout parameters and non-extensitivity. *Eur Phys J* (2025) 61:156. doi:10.1140/epja/s10050-025-01626-1

32. Patra N, Mohanty R, Nayak B, Centrality TK. Centrality, transverse momentum and collision energy dependence of the tsallis parameters in relativistic heavy-ion collisions. *Eur Phys J Plus* (2021) 136:702. doi:10.1140/epjp/s13360-021-01660-0

33. Kapusta JI. Perspective on tsallis statistics for nuclear and particle physics. *Int J Mod Phys E* (2021) 30(08):2130006. doi:10.1142/s021830132130006x

34. Zheng H, Zhu LL. Comparing the tsallis distribution with and without thermodynamical description in collisions. *Adv High Energy Phys* (2016) 2016:9632126. doi:10.1155/2016/9632126

35. Zheng H, Zhu LL. Can tsallis distribution fit all the particle spectra produced at RHIC and LHC? *Adv High Energy Phys* (2015) 2015:180491–9. doi:10.1155/2015/180491

36. Andronic A, Munzinger PB, Stachel J. The Horn, the hadron mass spectrum and the QCD phase diagram C the statistical model of hadron production in central nucleus-nucleus collisions. *Nucl Phys A* (2010) 834(1-4):237c–240c. doi:10.1016/j.nuclphysa.2009.12.048

37. Cleymans J, Lykasov GI, Parvan AS, Sorin AS, Teryaev OV, Worku D. Systematic properties of the tsallis distribution: energy dependence of parameters in high energy P–P collisions. *Phys Lett B* (2013) 723(4-5):351–4. doi:10.1016/j.physletb.2013.05.029